6720–6727 *Nucleic Acids Research, 2008, Vol. 36, No. 21* *Published online 23 October 2008*
doi:10.1093/nar/gkn745

PCNA stimulates catalysis by structure-specific nucleases using two distinct mechanisms: substrate targeting and catalytic step

Richard D. Hutton[1], Jennifer A. Roberts[1], J. Carlos Penedo[2] and Malcolm F. White[1,*]

[1]Centre for Biomolecular Sciences and [2]School of Physics, University of St Andrews, Fife KY16 9ST, UK

Received August 14, 2008; Revised October 2, 2008; Accepted October 3, 2008

ABSTRACT

The sliding clamp Proliferating Cell Nuclear Antigen (PCNA) functions as a recruiter and organizer of a wide variety of DNA modifying enzymes including nucleases, helicases, polymerases and glycosylases. The 5′-flap endonuclease Fen-1 is essential for Okazaki fragment processing in eukaryotes and archaea, and is targeted to the replication fork by PCNA. Crenarchaeal XPF, a 3′-flap endonuclease, is also stimulated by PCNA *in vitro*. Using a novel continuous fluorimetric assay, we demonstrate that PCNA activates these two nucleases by fundamentally different mechanisms. PCNA stimulates Fen-1 by increasing the enzyme's binding affinity for substrates, as suggested previously. However, PCNA activates XPF by increasing the catalytic rate constant by four orders of magnitude without affecting the K_M. PCNA may function as a platform upon which XPF exerts force to distort DNA substrates, destabilizing the substrate and/or stabilizing the transition state structure. This suggests that PCNA can function directly in supporting catalysis as an essential cofactor in some circumstances, a new role for a protein that is generally assumed to perform a passive targeting and organizing function in molecular biology. This could provide a mechanism for the exquisite control of nuclease activity targeted to specific circumstances, such as replication forks or damaged DNA with pre-loaded PCNA.

INTRODUCTION

The Proliferating Cell Nuclear Antigen (PCNA) is a ring-shaped protein that encircles DNA, acting as a sliding clamp or platform. PCNA is conserved in eukarya and archaea, and in bacteria the β subunit of DNA polymerase III plays an analogous role. PCNA is an essential component of the core processes of DNA replication, recombination and repair and cell-cycle control (1). PCNA is loaded onto DNA at the replication fork by the clamp loader Replication Factor C (RFC), and subsequently recruits a variety of proteins to the fork. The interaction between the 5′-flap endonuclease Fen-1 and PCNA is essential for the recruitment of Fen-1 to replication forks, where it catalyses Okazaki fragment processing. Photobleaching experiments have shown that PCNA persists for long periods at replication forks, whilst Fen-1 and DNA ligase associate and dissociate rapidly—consistent with the view that PCNA functions as a stable loading platform for DNA modification enzymes (2). Although Fen-1 is quite active in the absence of PCNA *in vitro*, disruption of the Fen-1:PCNA interaction leads to DNA replication defects and newborn lethality in mice (3). Disruption of the interaction between PCNA and mismatch repair (MMR) proteins using an oligopeptide abolishes MMR in an *in vitro* system (4). Similarly, disruption of PCNA:MMR protein interactions in *Saccharomyces cerevisiae* abolishes MMR in meiotic recombination *in vivo* (5). These observations emphasize the important role of PCNA *in vivo*.

PCNA is generally considered to function as a DNA-targeting factor, allowing non-sequence-specific enzymes, such as DNA polymerases, endonucleases, ligases, helicases, mismatch repair proteins and glycosylases to associate more closely with their DNA substrates [reviewed in (6,7)]. The trimeric structure of PCNA yields three potential binding sites for proteins, leading to the suggestion that PCNA may coordinate cellular processes by bringing consecutive enzymes in a DNA processing pathway together, for example, in the Okazaki fragment processing pathway where the nuclease Fen-1, DNA ligase and DNA polymerase can bind PCNA simultaneously (8). Covalent modification of PCNA by ubiquitination and sumolyation has been shown to play an important role in damage bypass pathways during replication in *S. cerevisiae*,

*To whom correspondence should be addressed. Tel: +44 1334 463432; Fax: +44 1334 462595; Email: mfw2@st-and.ac.uk
Present address:
Jennifer A. Roberts, Almac Sciences (Scotland), Elvingston Science Centre, East Lothian, UK

probably by changing the affinity of different DNA polymerases and repair factors for the clamp (9,10).

Whilst the eukaryotic PCNA protein is a homotrimer, in *Sulfolobus solfataricus* (and probably other crenarchaea) PCNA is heterotrimeric, with a tight association between subunits 1 and 2 and a much weaker interaction of the 1–2 heterodimer with subunit 3 that may facilitate DNA loading (8). The structure of the PCNA heterotrimer has been solved both on its own (11) and as a complex with Fen-1 (12,13) and DNA ligase (13), and closely resembles the euryarchaeal and eukaryotic homotrimeric protein structures. In addition to interactions with ligase, Fen-1, DNA polymerases and glycosylases, *S. solfataricus* PCNA stimulates the activities of the Holliday junction endonuclease Hjc (14) and the 3′-flap endonuclease XPF (15). We showed previously that PCNA stimulates the cleavage activity of XPF for a wide variety of DNA substrates to a remarkable degree (16,17). Here, we utilize a novel fluorescence resonance energy transfer (FRET) assay to demonstrate that PCNA stimulates Fen-1 and XPF in quite distinct ways. The activity of Fen-1 is increased primarily by lowering the K_M for substrates, as was shown previously for the human proteins (18). This represents the widely accepted DNA targeting model for PCNA activation. In sharp contrast, PCNA is an essential cofactor for the XPF nuclease, stimulating catalytic rates by almost 10 000-fold. This is achieved by increasing the maximal velocity of the DNA cleavage reaction, whilst K_M's for substrates are not affected. These data suggest that PCNA increases the catalytic rate constant by reducing the activation barrier of the cleavage reaction. This represents a novel role for the PCNA sliding clamp that may be relevant for other PCNA-dependent enzymes.

MATERIALS AND METHODS

Protein expression and purification

Sulfolobus solfataricus XPF and PCNA heterotrimer were expressed and purified as described previously (8,16). The *S. solfataricus fen-1* gene was amplified from *S. solfataricus* strain P2 genomic DNA using the following primers:

5′-primer:
5′-CGTCGGATCCCCATGGATTTAGCAGA-TTTAGTAAAAG
3′-primer:
5′-CCGGGGATCCGTCGACTTAAAACCA-TCTGTCCAATCCTGTTTGTC

The PCR product was cloned into the NcoI/BamHI sites of the vector pET28c (Novagen, Darmstadt, Germany) for native protein expression. Protein expression was carried out in BL21 Rosetta (DE3) cells induced by adding 0.2 mM IPTG when cultures reached A_{600} 0.7, grown for further 3 h and the cells pelleted. The bacterial pellet was resuspended in ~35 ml lysis buffer (20 mM MES pH 6.0, 1 mM EDTA, 0.5 mM DTT, 100 mM NaCl, 1 mM benzamidine) and sonicated for 4×2 min with cooling. The lysate was centrifuged at 48 000g for 20 min, 4°C and the supernatant heated to 70°C to precipitate *Escherichia coli* proteins before centrifugation for a further 20 min. The supernatant was filtered (Acrodisc 0.1 μM syringe filter, Pall Corporation, East Hills, NY, USA) and diluted 3-fold with buffer A (20 mM MES pH 6.0, 1 mM EDTA, 0.5 mM DTT). This was applied to a 5 ml Hitrap heparin column (GE Healthcare, Chalfont St Giles, UK) equilibrated with buffer A and the bound cationic proteins eluted over a 120 ml linear gradient of 0–1000 mM NaCl. The fractions containing Fen-1 were identified by SDS–PAGE, pooled and concentrated to ~7 ml and loaded onto a HiLoad® 26/60 Superdex® 200 gel filtration column (GE Healthcare) equilibrated with buffer (20 mM MES pH 6.0, 1 mM EDTA, 0.5 mM DTT, 150 mM NaCl). Fractions corresponding to the peak(s) were concentrated as before and the protein concentration calculated from the extinction coefficient at 280 nm (15). Protein was stored at −80°C in 15% glycerol until required.

Substrate formation

Unlabelled oligonucleotides used to make the DNA structures were purchased from Operon Biotechnologies GmbH (Cologne, Germany), the fluorescent oligonucleotides used were purchased from Integrated DNA Technologies (Coralville, USA). The 3′-flap and 5′-double-flap substrates were assembled using 0.1 OD of each strand (Table 1) and mixed with hybridization buffer (20 mM Tris–HCl pH 7.8, 25 mM NaCl). The sample was then heated at 93°C for 2 min followed by slow overnight cooling to 4°C. The substrate was purified on a 10% non-denaturing acrylamide gel at 110 V for 4 h at 4°C. Bands were visualized and cut by UV shadowing and then extracted from the gel using a overnight crush and soak protocol at 4°C (CSH Protocols; 2006; doi:10.1101/pdb.prot2936), followed by ethanol precipitation. The absorption spectrum from 650 nm to 220 nm was used to determine DNA concentration and labelling efficiency of the fluorescent dyes. In addition, the sequences of all oligonucleotides were selected to have predicted melting temperatures >55°C such that under reaction conditions the duplex structure was favoured.

Endonuclease assays

Multiple turnover nuclease reactions were assembled in 30 mM HEPES, pH 7.6, 40 mM KCl, 5% glycerol, 0.1 mg/ml bovine serum albumin with 25 nM labelled DNA substrate and 1 nM XPF dimer or FEN-1 monomer.

Table 1. Oligonucleotides used for DNA substrates

Oligo	Sequence (5′ to 3′)
XPFA	ACCGTCCG[dT-Fluo]CCTAGCAAGCATT[Cy3]
XPFB	TCTGACTGCAGTCGGGCT
XPFC	AGCCCGACAGCAGTCAGAGCTTGCTAGGACGGACGGT
FEN-1A	ACCTAGGTCCGTCCTAGCAAGCC
FEN-1B	[Cy3]TTATCTGACTGCAGTC[dT-Fluo]AGCTACTG
FEN-1C	CAGTAGCTAGACTGCAGTCAGAGCTTGCTAGGACGGACCTAGGT

Unlabelled DNA substrate and PCNA heterotrimer were added to the required concentration. When using short synthetic DNA substrates, PCNA can diffuse readily onto the DNA and there is no need for the addition of the clamp loader RFC. Reactions were equilibrated at 55°C for 10 min before the reaction was initiated, readings were then taken for 5 min so that a stable baseline was achieved. The reaction was initiated by the addition of $MgCl_2$ in 5% glycerol to a final concentration of 10 mM, and monitored to completion. To minimize evaporation a layer of mineral oil was added to prevent evaporation within the cell. Cleavage rates were calculated by fitting the raw data to a single exponential equation generating reaction start and end point values. The *Y*-axis was rescaled to reflect fmol product, and the reaction rate was obtained by linear regression (fmol product/min/fmol enzyme). Data were obtained in triplicate and fitted to the Michaelis–Menten equation by non-linear regression.

Experiments were performed on a Cary Eclipse spectrofluorimeter (Varian Inc., Palo Alto, USA) under magic angle conditions to avoid anisotropy artefacts on the fluorescence signal, equipped with a Peltier temperature controller set to 55°C. All samples were filtered before analysis and analyzed via a time base scan (λ_{ex} = 490 nm, λ_{em} = 520 nm) in a Suprasil quartz cuvette (10 mm path) in a total volume of 150 µl. Reactions were equilibrated to the incubation temperature before initiation of DNA cleavage as was evident by a steady background emission signal over 10 min. Total cleavage of the labelled oligonucleotide, confirmed by PAGE, was defined as the maximum fluorescence emission possible under saturated cleaving conditions. Emission units were converted to the amount of labelled oligonucleotide used within a procedure, thereby equating labelled oligonucleotide cleavage as a function of the emission of fluorescence. To achieve specific DNA substrate concentrations a constant 25 nM of labelled DNA was used and unlabelled DNA was added to the required concentration. Experiments were performed over a range of PCNA concentrations to study the effect of PCNA on the activity of XPF and Fen-1. single-turnover assays were carried out in the same way using the indicated concentrations of XPF or Fen-1.

Isothermal titration calorimetry

Binding of XPF or Fen-1 to PCNA was assessed by isothermal titration calorimetry (ITC) using a VP-ITC unit operating at 328 K for XPF and 293 K for Fen-1 (Microcal, GE Healthcare, Chalfont St Giles, UK). Before use, proteins were dialysed against binding buffer and degassed in a vacuum. All concentrations were measured by UV absorption immediately before titrations were started. For Fen-1, binding buffer was 30 mM HEPES pH 7.6, 40 mM KCl and titrations comprised 50 injections of Fen-1, one 2-µl injection followed by 49 5-µl injections. For XPF binding buffer was 50 mM Tris–HCl pH 7.4, 200 mM NaCl and titrations comprised 26 injections of XPF, one 2-µl injection followed by 25 10-µl injections. The initial data point was routinely deleted to allow for diffusion of ligand/receptor across the needle tip during the equilibration period. Heats of dilution experiments were measured independently and subtracted from the integrated data before curve-fitting in Origin 7.0 with the standard one site model supplied by MicroCal.

RESULTS

Quantification of XPF and Fen-1 binding to PCNA

Both *S. solfataricus* XPF and Fen-1 have been shown previously to interact with the heterotrimeric PCNA molecule in the absence of DNA, but binding affinities have not been measured. We used ITC to determine the dissociation constants of both proteins for PCNA in solution. Fen-1 bound to PCNA with a K_D of 210 ± 13 nM and a stoichiometry of 0.998 ± 0.002 Fen-1 monomer per PCNA trimer (Figure 1A). XPF bound to PCNA with a stoichiometry of 1.1 ± 0.2 XPF dimer per PCNA trimer and a K_D of 3.8 ± 0.6 µM (Figure 1B). By comparison, human PCNA interacts with the mismatch binding protein MutSα in solution with a 1:1 stoichiometry and a K_D of 0.7 µM (19).

Development of a continuous, fluorescence-based assay for XPF and Fen-1

Previous experiments on *S. solfataricus* XPF have utilized a discontinuous, single-turnover assay with a radiolabelled substrate (16). To facilitate analysis of multi-turnover kinetics with a continuous assay, we developed a FRET-based assay where the DNA strand targeted for cleavage has two dyes: a donor dye (fluorescein) located 5′ to the cleavage point and an acceptor dye (Cy3) located on the terminus of the 3′-flap (Table 1, Figure 2). The close proximity of the donor and acceptor groups in the same DNA strand facilitated efficient energy transfer thereby reducing fluorescence emission intensity from the donor moiety at 520 nm upon excitation at 490 nm (Figure 2B). Cleavage of the strand resulted in alleviation of this quenching and an increase in fluorescence emission intensity at 520 nm. The assay was based on a previously reported method (20). The expected cleavage products of the fluorescent construct were observed by separating the reaction products by denaturing gel electrophoresis and visualization by phosphorimaging (Fuji FLA5100, Fujifilm, Tokyo, Japan) using a SHG green laser (532 nm) to observe Cy3 fluorescence, confirming that substrate strand cleavage had taken place (Figure 2C).

A similar strategy was used to design a fluorescent substrate for Fen-1. The optimal double-flap substrate was chosen, which consists of an unpaired 3′-nucleotide and a 5′-ssDNA flap (21). The donor dye (fluorescein) was located 3′ of the cleavage point and the acceptor dye (Cy3) was located on the terminus of the 5′-flap on the same strand (Table 1, Figure 2A). Cleavage of the flap by Fen-1 resulted in an increase in fluorescence emission of the fluorescein reporter at 520 nM that could be followed in a continuous assay format as for XPF.

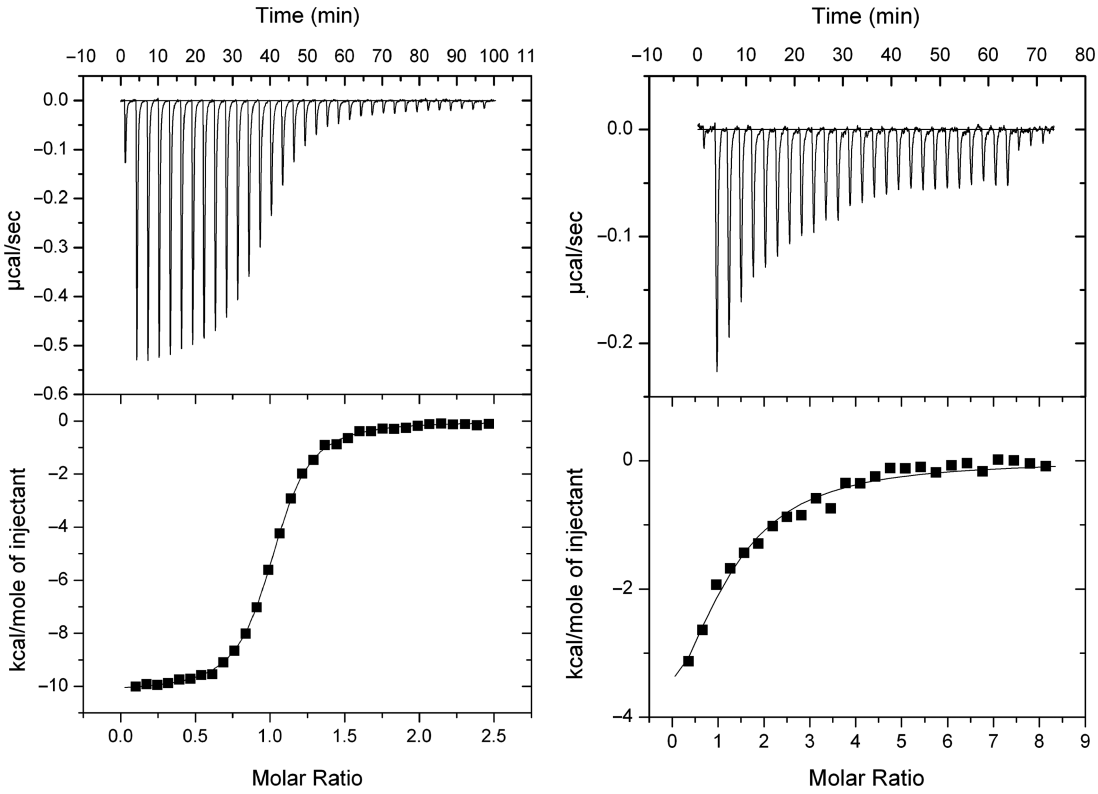

Figure 1. Interaction of PCNA with XPF and Fen-1 quantified by ITC. (**A**) Quantification of Fen-1 and PCNA interaction by ITC. Fen-1 (268 µM in the syringe) was injected into a solution of 13 µM PCNA heterotrimer at 293 K and heats of dilution monitored. The data were fitted with a simple one site binding model, yielding a K_D of 210 nM and a binding stoichiometry of 1:1. (**B**) Quantification of XPF and PCNA interaction by ITC. XPF (170 µM dimer in syringe) was injected into a solution of 4 µM PCNA heterotrimer at 328 K and heats of dilution monitored. The data were fitted with a simple one site binding model, yielding a K_D of 3.8 µM and a binding stoichiometry of 1:1.

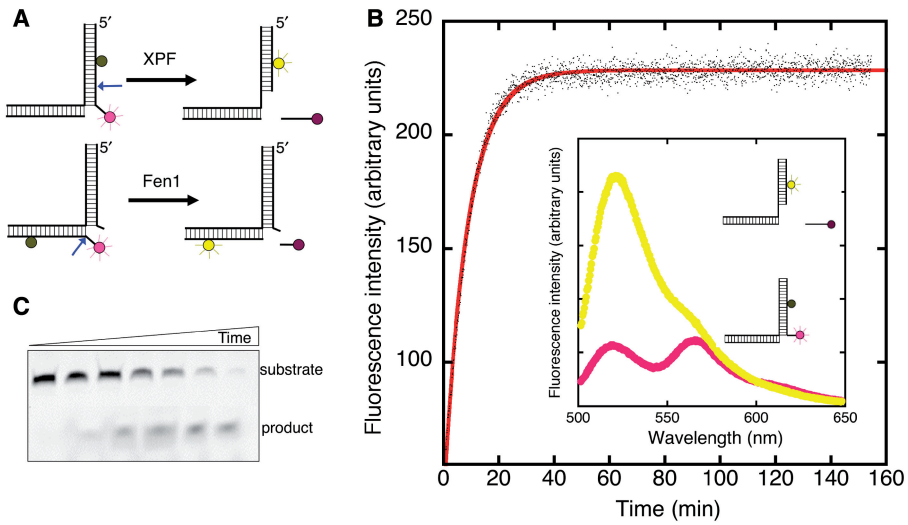

Figure 2. A continuous fluorescence assay for XPF and Fen-1. (**A**) Schematic showing design of steady-state FRET-based cleavage assays for XPF and Fen-1. Refer to Table 1 for the sequences. (**B**) Progress of the XPF substrate cleavage by the XPF–PCNA holoenzyme can been monitored by the increase in the donor (fluorescein) emission at 520 nm. The solid line represents the fitting of the experimental data to a single exponential model. Inset: change in the fluorescence emission spectrum (λ_{exc} 490 nm) observed upon substrate cleavage by XPF–PCNA. The emission spectrum before initiation of the reaction by addition of magnesium (pink), and (yellow) are shown. (**C**) Denaturing gel electrophoresis confirms that the fluorescent XPF substrate is cleaved by XPF–PCNA.

PCNA activates the catalytic step of XPF but not Fen-1

Single-turnover experiments were performed over a temperature range from 25°C to 55°C. The XPF concentration was 1 μM and DNA substrate concentration 80 nM. Data are shown graphically in Figure 3A and summarized in Table 2. Experiments performed at 55°C in the presence of 1 μM PCNA yielded a k_c value of 9.1 min^{-1}. This compares well with the rate of 6.8 min^{-1} estimated using a discontinuous radiation-based assay (16), giving confidence that the fluorescent labels did not interfere with catalysis by XPF. Experiments performed under identical conditions but without added PCNA yielded a k_c value of 1×10^{-3} min^{-1}, ~7000-fold less active than in the presence of PCNA (Figure 3B, Table 2). This is clear evidence that PCNA activates the catalytic cleavage activity of XPF, presumably by stabilizing the transition state or destabilizing the substrate. In marked contrast, single-turnover rate constants for Fen-1 in the presence and absence of 1 μM PCNA yielded highly similar k_c values of 10.3 min^{-1} and 10.6 min^{-1}, respectively, at 55°C, suggesting there is no intrinsic stimulation of the catalytic step of Fen-1 by PCNA (Figure 3B, Table 2). Both enzymes showed temperature-dependent kinetics as expected, with a 2- and 3-fold increase in catalytic rate for every 10°C increase in temperature for Fen-1 and XPF, respectively.

Steady-state kinetic analyses of XPF and Fen-1

The pre-steady-state rate constants measured for XPF highlighted the crucial role of PCNA in the activation of catalysis by this endonuclease, and confirmed previous measurements using discontinuous assays. The fluorescence-based assay allowed measurement of steady-state kinetics for XPF, which yield complementary information on the cycle of binding, catalysis and product release. Steady-state kinetic measurements of XPF were carried out by assaying 1 nM XPF and a DNA substrate concentration range of 25–650 nM at 55°C. Initial velocities at each substrate concentration (Figure 4A) were fitted to the Michaelis–Menten equation (Figure 4B) to yield kinetic constants k_{cat} and K_M. Steady-state experiments in the absence of PCNA showed no activity for XPF over a time period of 72 h. Inclusion of PCNA at concentrations from 50 nM to 20 μM increased the k_{cat} from 0.37 min^{-1} to 5.5 min^{-1} (Figure 4C), without changing the K_M which remained constant at 85 ± 10 nM at all concentrations of PCNA tested (Figure 4D). The close agreement between the catalytic rate constant k_c and the turnover number k_{cat}, 9.1 min^{-1} and 5.5 min^{-1}, respectively, suggests that the catalytic step, rather than substrate binding or product release by XPF, is rate-limiting. The variation of k_{cat} with PCNA concentration shown in Figure 4C yielded an apparent K_M of 4 ± 0.7 μM for XPF and PCNA. This was in good agreement with the K_D of 3.8 μM determined from the ITC experiment, reinforcing the conclusion that the PCNA–XPF complex is essential for nuclease activity.

Steady-state kinetic analysis was also carried out for Fen-1. As observed previously, Fen-1 activity was not strictly dependent on the presence of PCNA. An ~3-fold increase in k_{cat} from 2.6 min^{-1} to 7.3 min^{-1} was observed

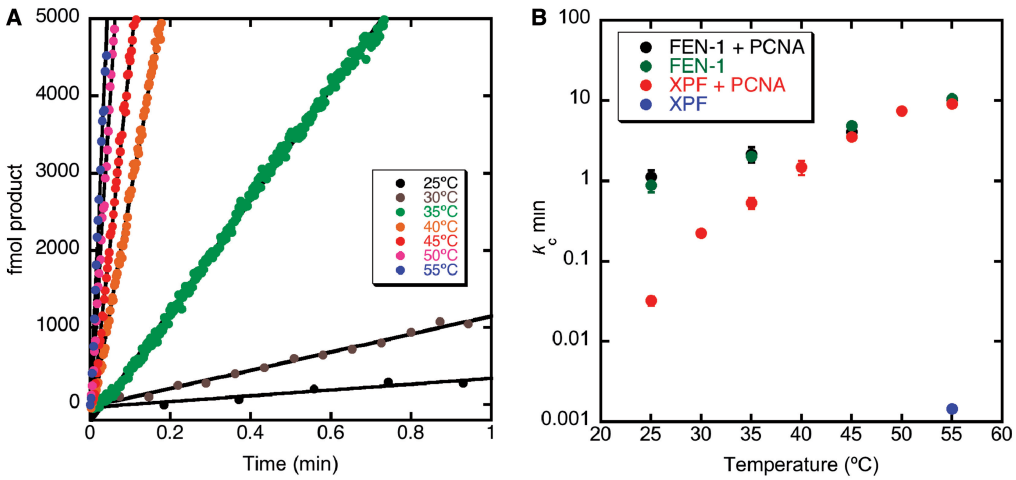

Figure 3. DNA substrate cleavage by XPF and Fen-1 in the presence and absence of PCNA. (**A**) Representative traces showing the continuous monitoring by FRET of DNA substrate cleavage and product formation by the XPF–PCNA complex at different temperatures under single-turnover conditions. (**B**) Variation in the catalytic rate constants for DNA substrate cleavage by 1 μM XPF or Fen-1 in the presence and absence of 10 μM PCNA as a function of temperature. Fen-1 is not significantly stimulated by PCNA under single-turnover conditions, whilst XPF is only marginally active in the absence of PCNA. Experiments were carried out in triplicate and means with standard errors are shown.

Table 2. Summary of kinetic parameters determined for XPF and Fen-1 in the presence and absence of PCNA

	k_c (min^{-1})	k_{cat} (min^{-1})	K_M (M)	k_{cat}/K_M (M^{-1} min^{-1})
XPF	$(1.0 \pm 0.2) \times 10^{-3}$	–	–	–
XPF + PCNA	9.1 ± 0.3	5.5 ± 0.2	$(93 \pm 8) \times 10^{-9}$	$(59 \pm 7) \times 10^{6}$
Fen-1	10.6 ± 0.9	2.6 ± 0.2	$(290 \pm 40) \times 10^{-9}$	$(9 \pm 2) \times 10^{6}$
Fen-1 + PCNA	10.3 ± 0.3	7.3 ± 0.3	$(67 \pm 10) \times 10^{-9}$	$(110 \pm 16) \times 10^{6}$

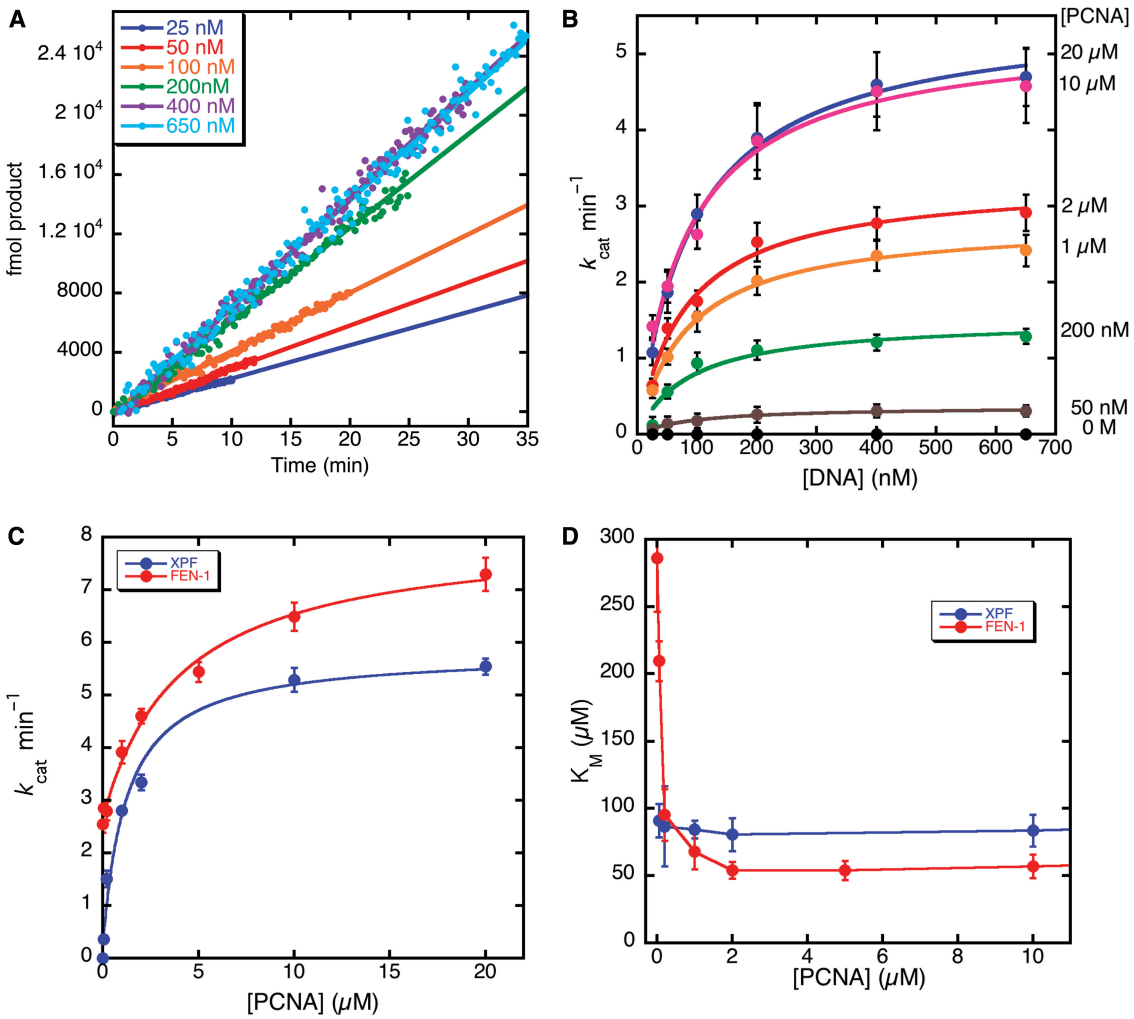

Figure 4. Multiple turnover kinetic analyses of XPF and Fen-1. (**A**) Representative data showing the reaction progress of multiple turnover catalysis of 1 nM XPF and 10 μM PCNA at 55°C with respect to DNA substrate concentration. (**B**) Plot showing the dependence of XPF catalytic rate on DNA concentration at a variety of PCNA concentrations from 0 μM to 20 μM. The data were fitted to the Michaelis–Menten equation. (**C**) Plot showing the variation in rate constant k_{cat} for XPF (blue) and Fen-1 (red) with respect to PCNA concentration. (**D**) Plot showing the variation in Michaelis constant K_M for XPF (blue) and Fen-1 (red) with respect to PCNA concentration. K_M values for XPF are not affected by alterations in PCNA concentration, whilst those for Fen-1 are strongly dependent on the concentration of PCNA. All data points in (B–D) are the means of triplicate experiments and standard errors are shown.

as the PCNA concentration increased from 0 μM to 20 μM (Figure 4C). In contrast to XPF, the K_M for Fen-1 was strongly dependent on PCNA concentration, dropping from 290 nM to 60 nM as PCNA increased from 0 μM to 5 μM (Figure 4D). Together with the single-turnover experiments, this suggests that the stimulatory effect of PCNA on Fen-1 is largely related to substrate binding.

DISCUSSION

Stimulation of Fen-1 by PCNA—substrate targeting

The sliding clamp PCNA binds to DNA and interacts with a wide variety of proteins. It is generally accepted that PCNA's function is to recruit a variety of DNA modification proteins to relevant DNA structures. This implies a rather passive role in catalysis, as a moderately stimulatory factor whose main function is in targeting and organization of components of quite complex molecular machines catalysing processes, such as DNA replication or MMR. Virtually all previously described PCNA-interacting proteins are reasonably active in the absence of PCNA. A good example is the 5′-flap endonuclease Fen-1, whose activity is only moderately stimulated by PCNA *in vitro*. Nevertheless, interactions with PCNA have been shown to be crucial for cell survival *in vivo* (3), emphasizing the role of PCNA as a molecular organizer or mediator.

Previously published kinetic studies of human and archaeal Fen-1's have reported widely divergent kinetic constants. In several instances, this has been complicated by reporting of multiple turnover rate constants and K_M's derived from assays where Fen-1 was equimolar to or in excess of the substrate concentration. Some Fen-1's seem to be highly sensitive to the presence of DTT for full

activity (22), and the pH used by different investigators has varied widely. The continuous fluorescent assay system we have reported here has clear advantages over discontinuous assays used previously. The single-turnover rate (k_c) for *S. solfataricus* Fen-1 of 10.3 min^{-1} was close to the multiple turnover k_{cat} of 7.3 min^{-1} suggesting that, as with XPF, the catalytic step is rate limiting under the multiple turnover conditions used in these experiments. This contrasts with the phage T5-flap endonuclease, where turnover rates are limited by product release rather than the catalytic step (22).

The k_{cat} for human Fen-1 in the absence of PCNA, with a double-flap substrate at pH 8.0, 37°C, is reported as 11 min^{-1} (23). The turnover number for *Archaeoglobus fulgidus* Fen-1 is reported to be considerably higher, about 100 min^{-1} with a similar substrate at pH 9.3, 55°C and a large increase in reaction rate was observed when 1 mM DTT was present in the reaction buffer (22). We observed no influence of DTT on the cleavage rate of *S. solfataricus* Fen-1, and note that whilst *A. fulgidus* Fen-1 has a single cysteine residue that may conceivably influence catalysis, *S. solfataricus* Fen-1 has no cysteines in its primary sequence. However, we did observe an ~10-fold increase in both the single- and multiple-turnover rate constants for *S. solfataricus* Fen-1 assayed at pH 9.3, bringing the catalytic constants close to those reported for *A. fulgidus* Fen-1 (22) (data not shown). In common with studies of other Fen-1 enzymes, we have shown that *S. solfataricus* Fen-1 is only moderately stimulated by PCNA and that this effect is mostly at the level of DNA binding. Under single-turnover conditions, PCNA has no effect on Fen-1 activity. Under steady-state conditions, the K_M of *S. solfataricus* Fen-1 for a double-flap substrate was reduced from 290 nM in the absence of PCNA to 60 nM at saturating concentrations of PCNA. By comparison, the K_M of *A. fulgidus* Fen-1 for a double-flap substrate was estimated at 1.4 μM in the absence of PCNA (22). In reactions carried out at pH 9.3, the effect of PCNA (20 μM) on *S. solfataricus* Fen-1 activity was qualitatively similar to that observed at pH 7.6, with a modest increase in V_{max} and a 4-fold decrease in K_M. This suggests that the mechanism by which PCNA stimulates Fen-1 is similar at both the high and low pH's, and is likely to be a general phenomenon for Fen-1's from different organisms.

Stimulation of XPF by PCNA—an essential cofactor for catalysis

In sharp contrast to the situation for Fen-1, the 3′-flap endonuclease XPF has a 7000-fold lower catalytic rate constant in the absence of PCNA. Under steady-state conditions, activity was undetectable in the absence of PCNA, and increasing concentrations of PCNA resulted in an increase k_{cat} but had no effect on K_M. These observations suggest strongly that the role of the sliding clamp in the XPF-mediated reaction is fundamentally different from that observed with Fen-1 and other DNA modification enzymes. Here, PCNA must be regarded as an essential cofactor or protein subunit of the XPF holoenzyme. In other words, the XPF:PCNA complex is the active entity. Consistent with this hypothesis, the variation of

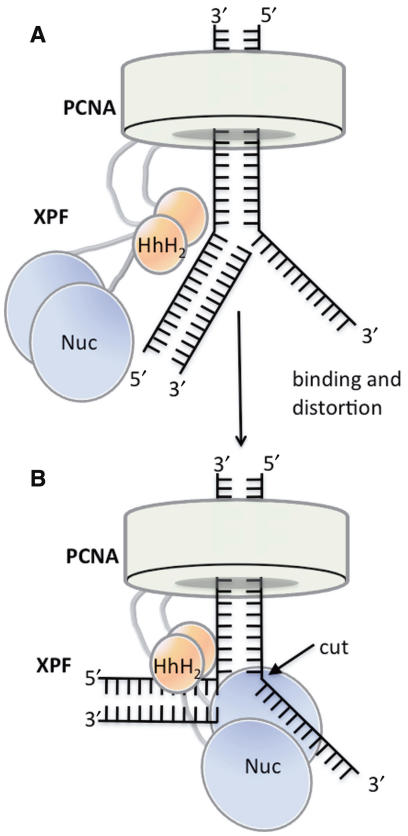

Figure 5. Scale cartoon showing a potential mechanism for PCNA activation of XPF endonuclease activity. (**A**) PCNA loaded onto duplex DNA can associate reversibly with the XPF endonuclease, which is composed of two dimeric domain joined by a flexible linker and binds to PCNA via a C-terminal PIP motif. (**B**) On encountering a suitable substrate for XPF, such as a 3′-flap, PCNA acts as a molecular fulcrum, providing a platform against which XPF can exert force to distort the DNA towards a productive structure for catalysis.

XPF k_{cat} with increasing PCNA concentration yields an apparent K_M for PCNA of 4 μM—in close agreement with the dissociation constant of the two proteins in solution measured by ITC at 3.8 μM.

Why is PCNA absolutely essential for catalysis by crenarchaeal XPF when its role in other situations is predominantly in substrate targeting and processivity? The XPF endonuclease is unusual in being organized with two dimeric domains joined by a flexible linker (24) (Figure 5). The C-terminal dimeric HhH_2 domain has a DNA-binding role, and is thought to distort DNA substrates, allowing the nuclease domain to remove the 3′-flap, or extend the gap upstream of a nicked DNA duplex. It is possible that PCNA functions as a molecular fulcrum in this situation; acting as a platform against which XPF can exert force to distort the DNA substrate and drive it towards the transition state (Figure 5B). This scenario can be viewed as a particular form of DNA targeting, as the XPF nuclease will only cleave substrates where PCNA is appropriately located *in vivo*. The activity of sequence non-specific nucleases must be controlled tightly *in vivo* to avoid non-specific DNA digestion. For example, cellular Holliday junction resolving enzymes are exquisitely specific for four-way DNA

junctions, whilst phage resolving enzymes, such as T4 endonuclease VII are more promiscuous and thus highly toxic when overexpressed in *E. coli* (25). The absolute dependence of XPF on PCNA for activity may therefore reflect an elegant control mechanism to limit the nuclease activity not only to particular DNA substrates, but to places such as replication forks where PCNA is loaded. This could ensure that subsequent PCNA-dependent reactions, such as DNA replication or ligation that are necessary following DNA cleavage by XPF are undertaken efficiently.

In summary, we have shown that the sliding clamp PCNA can stimulate catalysis by endonucleases by two quite different mechanisms. There may be other examples of apparently inactive nucleases that in fact have an absolute requirement for an interaction with the sliding clamp. Such mechanisms may ensure that nuclease activities are kept tightly regulated to prevent non-specific DNA cleavage.

ACKNOWLEDGEMENTS

Thanks to Uli Schwarz-Linek for help with the ITC experiments and to Joanna Somers for help in scanning fluorescent gels. Thanks to Biljana Petrovic-Stojanovska for technical support and the St Andrews University Mass Spectrometry facility for analyses.

FUNDING

Biotechnology and Biological Sciences Research Council (BBD0014391 and BBE0146741). Funding for open access charge: Biotechnology and Biological Research Council.

Conflict of interest statement. None declared.

REFERENCES

1. Warbrick,E. (2000) The puzzle of PCNA's many partners. *Bioessays*, **22**, 997–1006.
2. Sporbert,A., Domaing,P., Leonhardt,H. and Cardoso,M.C. (2005) PCNA acts as a stationary loading platform for transiently interacting Okazaki fragment maturation proteins. *Nucleic Acids Res.*, **33**, 3521–3528.
3. Zheng,L., Dai,H., Qiu,J., Huang,Q. and Shen,B. (2007) Disruption of the FEN-1/PCNA interaction results in DNA replication defects, pulmonary hypoplasia, pancytopenia, and newborn lethality in mice. *Mol. Cell. Biol.*, **27**, 3176–3186.
4. Masih,P.J., Kunnev,D. and Melendy,T. (2008) Mismatch repair proteins are recruited to replicating DNA through interaction with Proliferating Cell Nuclear Antigen (PCNA). *Nucleic Acids Res.*, **36**, 67–75.
5. Stone,J.E., Ozbirn,R.G., Petes,T.D. and Jinks-Robertson,S. (2008) Role of proliferating cell nuclear antigen interactions in the mismatch repair-dependent processing of mitotic and meiotic recombination intermediates in yeast. *Genetics*, **178**, 1221–1236.
6. Vivona,J.B. and Kelman,Z. (2003) The diverse spectrum of sliding clamp interacting proteins. *FEBS Lett.*, **546**, 167–172.
7. Moldovan,G.L., Pfander,B. and Jentsch,S. (2007) PCNA, the maestro of the replication fork. *Cell*, **129**, 665–679.
8. Dionne,I., Nookala,R.K., Jackson,S.P., Doherty,A.J. and Bell,S.D. (2003) A heterotrimeric PCNA in the hyperthermophilic archaeon Sulfolobus solfataricus. *Mol. Cell*, **11**, 275–282.
9. Hoege,C., Pfander,B., Moldovan,G.L., Pyrowolakis,G. and Jentsch,S. (2002) RAD6-dependent DNA repair is linked to modification of PCNA by ubiquitin and SUMO. *Nature*, **419**, 135–141.
10. Stelter,P. and Ulrich,H.D. (2003) Control of spontaneous and damage-induced mutagenesis by SUMO and ubiquitin conjugation. *Nature*, **425**, 188–191.
11. Williams,G.J., Johnson,K., Rudolf,J., McMahon,S.A., Carter,L., Oke,M., Liu,H., Taylor,G.L., White,M.F. and Naismith,J.H. (2006) Structure of the heterotrimeric PCNA from Sulfolobus solfataricus. *Acta crystallogr.*, **62**, 944–948.
12. Dore,A.S., Kilkenny,M.L., Jones,S.A., Oliver,A.W., Roe,S.M., Bell,S.D. and Pearl,L.H. (2006) Structure of an archaeal PCNA1-PCNA2-FEN1 complex: elucidating PCNA subunit and client enzyme specificity. *Nucleic Acids Res.*, **34**, 4515–4526.
13. Pascal,J.M., Tsodikov,O.V., Hura,G.L., Song,W., Cotner,E.A., Classen,S., Tomkinson,A.E., Tainer,J.A. and Ellenberger,T. (2006) A flexible interface between DNA ligase and PCNA supports conformational switching and efficient ligation of DNA. *Mol. Cell*, **24**, 279–291.
14. Dorazi,R., Parker,J.L. and White,M.F. (2006) PCNA activates the Holliday junction endonuclease Hjc. *J. Mol. Biol.*, **364**, 243–247.
15. Roberts,J.A., Bell,S.D. and White,M.F. (2003) An archaeal XPF repair endonuclease dependent on a heterotrimeric PCNA. *Mol. Microbiol.*, **48**, 361–371.
16. Roberts,J. and White,M.F. (2005) An archaeal endonuclease displays key properties of both eukaryal XPF-ERCC1 and Mus81. *J. Biol. Chem.*, **280**, 5924–5928.
17. Roberts,J.A. and White,M.F. (2005) DNA end-directed and processive nuclease activities of the archaeal XPF enzyme. *Nucleic Acids Res.*, **33**, 6662–6670.
18. Tom,S., Henricksen,L.A. and Bambara,R.A. (2000) Mechanism whereby proliferating cell nuclear antigen stimulates flap endonuclease 1. *J. Biol. Chem.*, **275**, 10498–10505.
19. Iyer,R.R., Pohlhaus,T.J., Chen,S., Hura,G.L., Dzantiev,L., Beese,L.S. and Modrich,P. (2008) The MutS{alpha}-proliferating cell nuclear antigen interaction in human DNA mismatch repair. *J. Biol. Chem.*, **283**, 13310–13319.
20. Ghosh,S.S., Eis,P.S., Blumeyer,K., Fearon,K. and Millar,D.P. (1994) Real time kinetics of restriction endonuclease cleavage monitored by fluorescence resonance energy transfer. *Nucleic Acids Res.*, **22**, 3155–3159.
21. Kaiser,M.W., Lyamicheva,N., Ma,W., Miller,C., Neri,B., Fors,L. and Lyamichev,V.I. (1999) A comparison of eubacterial and archaeal structure-specific 5′-exonucleases. *J. Biol. Chem.*, **274**, 21387–21394.
22. Williams,R., Sengerova,B., Osborne,S., Syson,K., Ault,S., Kilgour,A., Chapados,B.R., Tainer,J.A., Sayers,J.R. and Grasby,J.A. (2007) Comparison of the catalytic parameters and reaction specificities of a phage and an archaeal flap endonuclease. *J. Mol. Biol.*, **371**, 34–48.
23. Liu,R., Qiu,J., Finger,L.D., Zheng,L. and Shen,B. (2006) The DNA-protein interaction modes of FEN-1 with gap substrates and their implication in preventing duplication mutations. *Nucleic Acids Res.*, **34**, 1772–1784.
24. Newman,M., Murray-Rust,J., Lally,J., Rudolf,J., Fadden,A., Knowles,P.P., White,M.F. and McDonald,N.Q. (2005) Structure of an XPF endonuclease with and without DNA suggests a model for substrate recognition. *EMBO J.*, **24**, 895–905.
25. Lilley,D.M.J. and White,M.F. (2001) The junction-resolving enzymes. *Nat. Rev. Mol. Cell. Biol.*, **2**, 433–443.